Journal of Computational and Applied Mathematics 234 (2010) 1140–1152

Contents lists available at ScienceDirect

Journal of Computational and Applied Mathematics

journal homepage: www.elsevier.com/locate/cam

Pseudospectral methods for solving an equation of hypergeometric type with a perturbation

H. Alıcı *, H. Taşeli

Department of Mathematics, Middle East Technical University, 06531, Ankara, Turkey

ARTICLE INFO

Article history:
Received 15 September 2008
Received in revised form 22 May 2009

MSC:
33C45
34L40
65L60
65L15
81Q05

Keywords:
Schrödinger operator
Regular and singular Sturm–Liouville eigenvalue problems
Pseudospectral methods
Equation of hypergeometric type
Classical orthogonal polynomials

ABSTRACT

Almost all, regular or singular, Sturm–Liouville eigenvalue problems in the Schrödinger form

$$-\Psi''(x) + V(x)\Psi(x) = E\Psi(x), \quad x \in (\bar{a}, \bar{b}) \subseteq \mathbb{R},\ \Psi(x) \in L^2(\bar{a}, \bar{b})$$

for a wide class of potentials $V(x)$ may be transformed into the form

$$\sigma(\xi)y'' + \tau(\xi)y' + Q(\xi)y = -\lambda y, \quad \xi \in (a, b) \subseteq \mathbb{R}$$

by means of intelligent transformations on both dependent and independent variables, where $\sigma(\xi)$ and $\tau(\xi)$ are polynomials of degrees at most 2 and 1, respectively, and λ is a parameter. The last form is closely related to the equation of the hypergeometric type (EHT), in which $Q(\xi)$ is identically zero. It will be called here the equation of hypergeometric type with a perturbation (EHTP). The function $Q(\xi)$ may, therefore, be regarded as a perturbation. It is well known that the EHT has polynomial solutions of degree n for specific values of the parameter λ, i.e. $\lambda := \lambda_n^{(0)} = -n[\tau' + \frac{1}{2}(n-1)\sigma'']$, which form a basis for the Hilbert space $L^2(a, b)$ of square integrable functions. Pseudospectral methods based on this natural expansion basis are constructed to approximate the eigenvalues of EHTP, and hence the energies E of the original Schrödinger equation. Specimen computations are performed to support the convergence numerically.

1. Introduction

There has been a constant interest in the numerical solution of Sturm–Liouville eigenvalue problems, especially the one-dimensional Schrödinger equation described by the Hamiltonian

$$\mathcal{H} = -\frac{\mathrm{d}^2}{\mathrm{d}x^2} + V(x), \quad x \in (\bar{a}, \bar{b}),\ -\infty \le \bar{a} < \bar{b} \le \infty \tag{1}$$

for a variety of quantum mechanical potentials $V(x)$. Several approximation methods have been proposed for computing the eigenvalues of the problem by numerous researchers. Among these we may recall shooting methods [1], Prüfer transformation followed by a shooting procedure [2,3], constant perturbation methods [4,5], finite difference methods [6,7], variational methods [8–10], the Wronskian approach [11], the Hill determinant method [12–14], WKB and JWKB approximations [15–20], the recursive series method [21], the path-integral approach [22] and pseudospectral methods such as the quadrature discretization method [23,24] and pseudospectral methods based on classical orthogonal polynomials [25–27].

* Corresponding author.
E-mail addresses: ahaydar@metu.edu.tr (H. Alıcı), taseli@metu.edu.tr (H. Taşeli).

0377-0427/$ – see front matter © 2009 Elsevier B.V. All rights reserved.
doi:10.1016/j.cam.2009.06.004

The so-called Liouville's transformations reduce the classical Sturm–Liouville eigenvalue problems to the Schrödinger form. In general, because of its simple structure, authors would rather approximate the Sturm–Liouville eigenvalue problems in the Schrödinger form. However, in contrast, Taşeli and Alıcı [25] transformed the Schrödinger equation over the real line

$$\mathcal{H}\Psi(x) = E\Psi(x), \quad x \in (-\infty, \infty), \ \Psi \in L^2(-\infty, \infty) \tag{2}$$

into a more complicated but beneficial form

$$y'' - 2\xi y' + \left[\xi^2 - c^{-2}V\left(c^{-1}\xi\right)\right]y = \left[1 - c^{-2}E\right]y, \quad \xi \in (-\infty, \infty) \tag{3}$$

having a regular solution $y(\xi)$ in the new independent variable ξ. Furthermore, for a symmetric potential $V(x) := v(x^2)$, they showed that another pair of special transformations lead to two similar equations

$$\xi y'' + (\gamma + 1 - \xi)y' + \frac{1}{4}\left[\xi - c^{-2}v(c^{-2}\xi)\right]y = \frac{1}{4}\left[2(\gamma + 1) - c^{-2}E\right]y, \quad \xi \in (0, \infty) \tag{4}$$

on the half-line for the treatment of even ($\gamma = -1/2$) and odd ($\gamma = 1/2$) states of (2), separately [26]. Here c appears to be a scaling parameter. One, with a closer look, can easily see that (3) and (4) resemble Hermite

$$y'' - 2\xi y' = -2ny, \quad n \in \mathbb{N} \tag{5}$$

and Laguerre

$$\xi y'' + (\gamma + 1 - \xi)y' = -ny, \quad \gamma > -1, \quad n \in \mathbb{N} \tag{6}$$

equations, respectively, especially when the modified potentials $\xi^2 - c^{-2}V\left(c^{-1}\xi\right)$ and $\frac{1}{4}\left[\xi - c^{-2}v(c^{-2}\xi)\right]$ are viewed as perturbations on the zero potential. Thus, they conclude that the Hermite basis $\{H_n(\xi)\}$ for a general potential and the Laguerre basis $\{L_n^{\gamma}(\xi)\}$ with $\gamma = \pm 1/2$ for a symmetric potential are the most appropriate choices for a pseudospectral approximation of (2).

In this article, we generalize this idea to the Schrödinger equation defined over an arbitrary subset of the real line. To this end, we consider instead of specific cases such as (5) and (6) the unperturbed case as the general EHT

$$\sigma(\xi)y'' + \tau(\xi)y' = -\lambda^{(0)}y, \quad \xi \in (a, b) \subseteq \mathbb{R} \tag{7}$$

leading not only to the Hermite and Laguerre but also the Jacobi polynomials as well. Therefore, in Section 2, we show that besides (2), certain eigenvalue problems of physical and practical interest can indeed be reduced to the form

$$\sigma(\xi)y'' + \tau(\xi)y' + Q(\xi)y = -\lambda y, \quad \xi \in (a, b) \subseteq \mathbb{R} \tag{8}$$

which we have called the EHTP. Clearly, (3) and (4) are now particular cases of (8) in this setting. In Section 3, we then construct a very general pseudospectral formulation of the EHTP based on any polynomial solutions of the EHT including every possible selection of $\sigma(\xi)$ and $\tau(\xi)$. Section 4 is concerned with the construction of a general algorithm to determine the zeros of classical orthogonal polynomials. The last section concludes the paper with numerical examples and remarks.

2. Transformation into EHTP

Excluding a few degenerate cases such as that of quadratic σ with a double root, any EHT can be transformed into a Hermite (5), Laguerre (6) or Jacobi

$$(1 - \xi^2)y'' + [\beta - \alpha - (\alpha + \beta + 2)\xi]y' = -n(n + \alpha + \beta + 1)y, \quad \alpha, \beta > -1, \ n \in \mathbb{N} \tag{9}$$

differential equation by simple scaling and shifting operations; these are called the canonical forms [28]. Accordingly, Eq. (8) with $\sigma(\xi) = 1, \xi$ and $1 - \xi^2$ will be called here the EHTP of the first, second and the third kind, respectively. Therefore, the associated unperturbed cases, that is, EHTs in (5), (6) and (9), admit the classical orthogonal polynomials as their solutions, i.e. the Hermite polynomials $H_n(\xi)$, Laguerre polynomials $L_n^{\gamma}(\xi)$ of order γ and the Jacobi polynomials $P_n^{(\alpha,\beta)}(\xi)$ of order α and β, corresponding to the three kinds of problems.

We deal with, as a first example of the second kind, the radial Schrödinger equation

$$\left[-\frac{\mathrm{d}^2}{\mathrm{d}r^2} - \frac{M - 1}{r}\frac{\mathrm{d}}{\mathrm{d}r} + \frac{\ell(\ell + M - 2)}{r^2} + V(r)\right]\mathcal{R}(r) = E\mathcal{R}(r), \quad r \in (0, \infty), \tag{10}$$

which is naturally defined over the half-line so that $\mathcal{R}(r) \in L^2(0, \infty)$. Here, $M = 1, 2, \ldots$ and $\ell = 0, 1, \ldots$ are the space dimension and angular quantum number, respectively, and $V(r)$ is an arbitrary potential regular at the origin. Note that the Hamiltonian in (1), when considered over the half-line, is the particular case of (10) with $M = 1$ and $\ell = 0$ or $\ell = 1$. First introducing the scaled quadratic variable

$$\xi = (cr)^2, \quad c > 0, \ \xi \in (0, \infty) \tag{11}$$

we get the operational equivalences

$$\frac{1}{r}\frac{\mathrm{d}}{\mathrm{d}r} \equiv 2c^2\frac{\mathrm{d}}{\mathrm{d}\xi} \quad \text{and} \quad \frac{\mathrm{d}^2}{\mathrm{d}r^2} \equiv 4c^2\xi\frac{\mathrm{d}^2}{\mathrm{d}\xi^2} + 2c^2\frac{\mathrm{d}}{\mathrm{d}\xi} \tag{12}$$

for the first and second derivatives, respectively, so Eq. (10) reads as

$$\left[-\xi\frac{\mathrm{d}^2}{\mathrm{d}\xi^2} - \frac{M}{2}\frac{\mathrm{d}}{\mathrm{d}\xi} + \frac{\ell(\ell+M-2)}{4\xi} + \frac{1}{4c^2}V(c^{-1}\sqrt{\xi})\right]\mathcal{R}(\xi) = \frac{E}{4c^2}\mathcal{R}(\xi). \tag{13}$$

Then, proposing a solution of the type

$$\mathcal{R}(\xi) = \xi^{\ell/2}\mathrm{e}^{-\xi/2}y(\xi) \tag{14}$$

satisfying the asymptotic boundary condition at infinity and the regularity condition at the origin, we end up with an EHTP of the second kind

$$\xi y'' + \left(\frac{1}{2}M + \ell - \xi\right)y' + \frac{1}{4}\left[\xi - c^{-2}V(c^{-1}\sqrt{\xi})\right]y = \frac{1}{4}\left(M + 2\ell - c^{-2}E\right)y \tag{15}$$

where $y(\xi)$ should be regular. Note that the perturbation $Q(\xi)$ and the γ parameter in (6) are

$$Q(\xi) = \frac{1}{4}\left[\xi - c^{-2}V(c^{-1}\sqrt{\xi})\right] \quad \text{and} \quad \gamma = \frac{1}{2}M + \ell - 1 \tag{16}$$

respectively.

Next, as a second example, we consider the angular part of the internal amplitude function

$$\mathcal{T}\Theta(\theta; m) = E\Theta(\theta; m), \quad \theta \in \left(-\frac{1}{2}\pi, \frac{1}{2}\pi\right), \ \Theta(\theta; m) \in L^2\left(-\frac{1}{2}\pi, \frac{1}{2}\pi\right) \tag{17}$$

described by the trigonometric Hamiltonian

$$\mathcal{T} = -\frac{1}{\cos\theta}\frac{\mathrm{d}}{\mathrm{d}\theta}\left(\cos\theta\frac{\mathrm{d}}{\mathrm{d}\theta}\right) + \frac{m^2}{\cos^2\theta} + V(\sin^2\theta), \quad m = 0, 1, \ldots \tag{18}$$

where m stands for the magnetic quantum number. This problem results in a Schrödinger equation of a two-particle system by separation of variables under the assumption that the potential energy of the system is to be the sum of a central potential depending only on r and an angular potential which is a polynomial in even powers of $\sin\theta$ [29]. Singularities of (17) as well as the unboundedness of the trigonometric potential at $\theta = \pm\frac{1}{2}\pi$ imply that the eigenfunction Θ must vanish at the boundaries. Clearly, such an eigenfunction will be in the space $L^2(-\frac{1}{2}\pi, \frac{1}{2}\pi)$ of the square integrable functions which suggests the use of the Dirichlet conditions $\Theta(\pm\frac{1}{2}\pi; m) = 0$ at the boundaries. Furthermore, the reflection symmetry of the system under the replacement of θ by $-\theta$ implies that the spectrum can be decomposed into two subsets containing solely the even and odd states such that the corresponding eigenfunctions are even and odd functions of θ, respectively. For even states, introduction of the mapping

$$\xi = \cos 2\theta, \quad \xi \in (-1, 1), \tag{19}$$

which is not one-to-one, leads to the operational equivalences

$$\tan\theta\frac{\mathrm{d}}{\mathrm{d}\theta} \equiv -2(1-\xi)\frac{\mathrm{d}}{\mathrm{d}\xi} \quad \text{and} \quad \frac{\mathrm{d}^2}{\mathrm{d}\theta^2} \equiv 4(1-\xi^2)\frac{\mathrm{d}^2}{\mathrm{d}\xi^2} - 4\xi\frac{\mathrm{d}}{\mathrm{d}\xi} \tag{20}$$

which transform (17) into the form

$$\left[(1-\xi^2)\frac{\mathrm{d}^2}{\mathrm{d}\xi^2} + \left(\frac{1}{2} - \frac{3}{2}\xi\right)\frac{\mathrm{d}}{\mathrm{d}\xi} - \frac{m^2}{2(1+\xi)} - \frac{1}{4}V\left(\sqrt{\frac{1}{2}(1-\xi)}\right)\right]\Theta_e(\xi; m) = -\frac{1}{4}E\Theta_e(\xi; m) \tag{21}$$

subject to the condition $\Theta_e(-1; m) = 0$ for all m, where $\Theta_e(\xi; m)$ stands for an even eigenfunction in the original variable θ when ξ is replaced by $\cos 2\theta$. Next, to avoid the use of the term proportional to $(1+\xi)^{-1}$, we suggest an eigenfunction of the type

$$\Theta_e(\xi; m) = (1+\xi)^{m/2}y(\xi) \tag{22}$$

satisfying the above boundary condition as long as the new dependent variable y remains bounded at $\xi = -1$, to arrive at the EHTP of the third kind

$$(1-\xi^2)y'' + \left[m + \frac{1}{2} - \left(m + \frac{3}{2}\right)\xi\right]y' - \frac{1}{4}V\left(\sqrt{\frac{1}{2}(1-\xi)}\right)y = \frac{1}{4}[m(m+1) - E]y \tag{23}$$

with $\alpha = -\frac{1}{2}$ and $\beta = m$. It is not difficult to see that the last equation yields even states of (17) on returning back to the original variable θ via (22) and (19). On the other hand, odd state eigenfunctions can be expressed in the form

$$\Theta_o(\theta; m) = \sin\theta\Phi(\theta; m) \tag{24}$$

where Φ is necessarily an even function of θ. After straightforward manipulations, we see that Φ satisfies the equation

$$\left[-\frac{\mathrm{d}^2}{\mathrm{d}\theta^2} + (\tan\theta - 2\cot\theta)\frac{\mathrm{d}}{\mathrm{d}\theta} + \frac{m^2}{\cos^2\theta} + 2 + V(\sin\theta)\right]\Phi(\theta; m) = E\Phi(\theta; m), \quad \Phi\left(\pm\frac{1}{2}\pi\right) = 0. \tag{25}$$

The evenness of Φ implies the application of the same transformations (19) and (22), that is, $\xi = \cos 2\theta$ and $\Phi(\xi; m) = (1+\xi)^{m/2}y(\xi)$ which have been used for even states. Thus, we again reach at the EHTP of the third kind

$$(1-\xi^2)y'' + \left[m - \frac{1}{2} - \left(m + \frac{5}{2}\right)\xi\right]y' - \frac{1}{4}V\left(\sqrt{\frac{1}{2}(1-\xi)}\right)y = \frac{1}{4}[(m+1)(m+2) - E]y \tag{26}$$

but this time with $\alpha = \frac{1}{2}$ and $\beta = m$ which gives rise to odd states of (17).

The number of singular examples over a finite interval can be further increased. For instance, we have the equation

$$\left[-\frac{\mathrm{d}^2}{\mathrm{d}\theta^2} + \frac{\mu(\mu+1)}{2(1+\cos\theta)} + V(\cos\theta)\right]\Theta(\theta; \mu) = E\Theta(\theta; \mu), \quad \mu > 0,\ \theta \in (-\pi, \pi) \tag{27}$$

whose square integrable exact solutions $\Theta(\theta; \mu)$ have been examined in [30,31] when the regular part $V(\cos\theta)$ of the total potential is zero. Both the singularities and reflection symmetric structure of the system suggest the use of a procedure similar to that of (17). To be concise we omit the details of the transformations after which we obtain two similar EHTPs

$$(1-\xi^2)y'' + [\mu + 1 - (\mu+2)\xi]y' - V(\xi)y = \left[\frac{1}{4}(\mu+1)^2 - E\right]y \tag{28}$$

and

$$(1-\xi^2)y'' + [\mu - (\mu+3)\xi]y' - V(\xi)y = \left[\frac{1}{4}(\mu+2)^2 - E\right]y \tag{29}$$

of the third kind for the even ($\alpha = -\frac{1}{2}, \beta = \mu + \frac{1}{2}$) and odd ($\alpha = \frac{1}{2}, \beta = \mu + \frac{1}{2}$) states, respectively. So far we have just verified that a wide class of regular or singular eigenvalue problems can be treated by means of an EHTP. The next section introduces the general pseudospectral formulation in this frame.

3. Pseudospectral formulation of the EHTP

Roughly speaking, a pseudospectral method, also known as a spectral collocation method, is based on the Nth-degree polynomial interpolation of a function $y(\xi)$ denoted by $P_N(\xi)$,

$$P_N(\xi) = \sum_{n=0}^{N} \ell_n(\xi)y_n, \tag{30}$$

where the $y_n = y(\xi_n)$ are the actual values of $y(\xi)$ at the specified nodes $\xi = \xi_n$ for $n = 0, 1, \ldots, N$ [32]. The set of Lagrange interpolating polynomials $\{\ell_n(\xi)\}$ of degree N is defined by

$$\ell_n(\xi) = \frac{\pi(\xi)}{(\xi - \xi_n)\pi'(\xi_n)} \tag{31}$$

for each $n = 0, 1, \ldots, N$, in which

$$\pi(\xi) = \kappa\prod_{m=0}^{N}(\xi - \xi_m) \tag{32}$$

stands for a polynomial of degree $N+1$ with the real and distinct roots at the nodes. The Lagrange polynomials have the very well-known cardinality property $\ell_n(\xi_m) = \delta_{mn}$ where δ_{mn} is Kronecker's delta. As a result, both the interpolant $P_N(\xi)$ and the function $y(\xi)$ agree, at least at the nodes, $y(\xi_n) = P_N(\xi_n)$. Although the normalization constant κ is theoretically unnecessary, it plays a remarkable role in the numerical algorithm.

It is also possible to approximate the derivatives of the function $y(\xi)$ by differentiating the interpolant $P_N(\xi)$. Furthermore, the derivative values at the nodes ξ_n may be determined in terms of function values $y_n = P_N(\xi_n)$ by means of a *differentiation matrix* defined by

$$\boldsymbol{D}^{(k)} := [d_{mn}^{(k)}] = \frac{\mathrm{d}^k}{\mathrm{d}\xi^k}[\ell_n(\xi)]\bigg|_{\xi=\xi_m}, \quad k = 1, 2, \ldots, N \tag{33}$$

for $m, n = 0, 1, \ldots, N$. The approximate derivative values $\boldsymbol{y}^{(k)} = \left[P_N^{(k)}(\xi_0), P_N^{(k)}(\xi_1), \ldots, P_N^{(k)}(\xi_N)\right]^{\mathrm{T}}$ may therefore be written in matrix–vector form

$$\boldsymbol{y}^{(k)} = \boldsymbol{D}^{(k)}\boldsymbol{y} \tag{34}$$

where $\boldsymbol{y} = [y_0, y_1, \ldots, y_N]^{\mathrm{T}}$ is the vector of function values at the nodes. In particular, the entries of the first-order and the second-order differentiation matrices are defined by

$$d_{mn}^{(1)} = \frac{1}{2}\begin{cases} \dfrac{2\,\pi'(\xi_m)}{(\xi_m - \xi_n)\pi'(\xi_n)} & \text{if } m \neq n \\ \dfrac{\pi''(\xi_n)}{\pi'(\xi_n)} & \text{if } m = n \end{cases} \tag{35}$$

and

$$d_{mn}^{(2)} = \frac{1}{3}\begin{cases} \dfrac{3}{\xi_m - \xi_n}\left[\dfrac{\pi''(\xi_m)}{\pi'(\xi_n)} - 2d_{mn}^{(1)}\right] & \text{if } m \neq n \\ \dfrac{\pi'''(\xi_n)}{\pi'(\xi_n)} & \text{if } m = n \end{cases} \tag{36}$$

respectively [32,25].

Let us denote the classical orthogonal polynomial solutions of the EHT by $y(\xi) = p_n(\xi)$ corresponding to the values

$$\lambda_n^{(0)} = -n\left[\tau' + \frac{1}{2}(n-1)\sigma''\right] \tag{37}$$

of $\lambda^{(0)}$ for $n = 0, 1, \ldots$. Each $p_n(\xi)$ has exactly n real and distinct zeros which are interlaced [28], i.e. sorting all the roots in ascending order, the roots of $p_{n+1}(\xi)$ alternate with those of $p_n(\xi)$, so it obeys the definition of $\pi(\xi)$ in (32). Therefore, setting

$$\pi(\xi) = \kappa\prod_{m=0}^{N}(\xi - \xi_m) = p_{N+1}(\xi) \tag{38}$$

to be the polynomial solution $p_{N+1}(\xi)$ of the EHT, we define, from (35), the first-order differentiation matrix

$$d_{mn}^{(1)} = \frac{1}{2}\begin{cases} \dfrac{2}{\xi_m - \xi_n}\dfrac{p'_{N+1}(\xi_m)}{p'_{N+1}(\xi_n)} & \text{if } m \neq n \\ -\dfrac{\tau(\xi_n)}{\sigma(\xi_n)} & \text{if } m = n \end{cases} \tag{39}$$

in which the main diagonal entries have been simplified by using the fact that $p_{N+1}(\xi)$ satisfies the EHT in (7). Similarly, after some algebra, the elements of the second-order differentiation matrix in (36) take the form

$$d_{mn}^{(2)} = \frac{1}{3}\begin{cases} -\dfrac{3}{\xi_m - \xi_n}\left[\dfrac{\tau(\xi_m)}{\sigma(\xi_m)} + \dfrac{2}{\xi_m - \xi_n}\right]\dfrac{p'_{N+1}(\xi_m)}{p'_{N+1}(\xi_n)} & \text{if } m \neq n \\ \dfrac{1}{\sigma(\xi_n)}\left\{\dfrac{\tau(\xi_n)}{\sigma(\xi_n)}\left[\sigma'(\xi_n) + \tau(\xi_n)\right] + N\left[\tau' + \dfrac{1}{2}(N+1)\sigma''\right]\right\} & \text{if } m = n \end{cases} \tag{40}$$

with the help of (7) and (37). Higher order differentiation matrices may be obtained in a similar manner; however, first-order and second-order differentiation matrices are sufficient for a treatment of a second-order differential operator.

Now the interpolant $P_N(\xi)$ in (30) is proposed to be an approximate solution of the EHTP, where N may be regarded as the approximation or truncation order. Therefore, we require that the EHTP is satisfied at the nodal points ξ_m

$$\sum_{n=0}^{N}\left[\sigma(\xi_m)\ell_n''(\xi_m) + \tau(\xi_m)\ell_n'(\xi_m) + Q(\xi_m)\ell_n(\xi_m)\right]y_n = -\lambda\sum_{n=0}^{N}\ell_n(\xi_m)y_n \tag{41}$$

for $m = 0, 1, \ldots, N$ leading to the discrete representation

$$\widehat{\boldsymbol{\mathcal{B}}}\boldsymbol{y} = -\lambda\boldsymbol{y} \tag{42}$$

of the differential eigenvalue problem. Here, the vector $\boldsymbol{y} = [y_0, y_1, \ldots, y_N]^{\mathrm{T}}$ involves the values of an eigensolution at the nodal points, and the general entry $\widehat{\mathcal{B}}_{mn}$ of the matrix $\widehat{\boldsymbol{\mathcal{B}}} = [\widehat{\mathcal{B}}_{mn}]$ is given by

$$\widehat{\mathcal{B}}_{mn} = \sigma(\xi_m)d_{mn}^{(2)} + \tau(\xi_m)d_{mn}^{(1)} + Q(\xi_m)\delta_{mn}, \qquad m, n = 0, 1, \ldots, N. \tag{43}$$

By using (39) and (40) the first two terms in (43) can be incorporated to define

$$\widehat{\mathcal{K}}_{mn} := \sigma(\xi_m)d^{(2)}_{mn} + \tau(\xi_m)d^{(1)}_{mn} = \begin{cases} \dfrac{-2\sigma(\xi_m)}{(\xi_m-\xi_n)^2}\,\dfrac{p'_{N+1}(\xi_m)}{p'_{N+1}(\xi_n)} & \text{if } m \neq n \\ \dfrac{\tau(\xi_n)}{6\sigma(\xi_n)}\left[2\sigma'(\xi_n)-\tau(\xi_n)\right] + \dfrac{1}{3}N\left[\tau' + \dfrac{1}{2}(N+1)\sigma''\right] & \text{if } m = n \end{cases} \tag{44}$$

which represents the effect of kinetic energy terms independent of a specified potential.

It seems that the evaluation of $\widehat{\mathcal{K}}_{mn}$ requires the computation of the derivatives $p'_{N+1}(\xi_n)$ of the classical orthogonal polynomials at the nodes. Fortunately, a nice similarity transformation $\boldsymbol{\mathcal{B}} = \boldsymbol{S}^{-1}\widehat{\boldsymbol{\mathcal{B}}}\boldsymbol{S}$ in which $\boldsymbol{S} = \mathrm{diag}\{s_0, s_1, \ldots, s_m, \ldots, s_N\}$ with

$$s_m = \sqrt{\sigma(\xi_m)}p'_{N+1}(\xi_m), \quad m = 0, 1\ldots, N \tag{45}$$

makes it possible to avoid such onerous labor. Furthermore, the matrix in (42) reduces to a symmetric one, say $\boldsymbol{\mathcal{B}} = \boldsymbol{S}^{-1}(\widehat{\boldsymbol{\mathcal{K}}} + \boldsymbol{Q})\boldsymbol{S}$, whose entries are given by

$$\mathcal{B}_{mn} = \mathcal{K}_{mn} + Q_m\delta_{mn} \tag{46}$$

where

$$\mathcal{K}_{mn} = -\frac{1}{6}\begin{cases} \dfrac{12\sqrt{\sigma(\xi_m)\sigma(\xi_n)}}{(\xi_m-\xi_n)^2} & \text{if } m \neq n \\ \dfrac{\tau(\xi_n)}{\sigma(\xi_n)}\left[\tau(\xi_n) - 2\sigma'(\xi_n)\right] - 2N\left[\tau' + \dfrac{1}{2}(N+1)\sigma''\right] & \text{if } m = n \end{cases} \tag{47}$$

and $\boldsymbol{Q} = [Q_m\delta_{mn}]$ with $Q_m = Q(\xi_m)$. Thus, the eigenvalues of (42), and, hence, the approximate eigenvalues of the EHTP can be determined by the symmetric matrix eigenvalue problem

$$\boldsymbol{\mathcal{B}}\boldsymbol{u} = -\lambda\boldsymbol{u} \tag{48}$$

since the similar matrices participate of the same spectrum. The construction of the resulting symmetric, square matrix $\boldsymbol{\mathcal{B}}$ of size $N+1$ can be accomplished by the calculation of the coefficient functions $\sigma(\xi)$, $\tau(\xi)$ and $Q(\xi)$ in EHTP (8) at the nodes. Therefore, it remains only to determine the roots ξ_m of the appropriate classical orthogonal polynomial $p_{N+1}(\xi)$ employed in the set-up of the Lagrange interpolating polynomials. Recall that $p_{N+1}(\xi)$ is the polynomial solution of degree $N+1$ of the associated EHT in (7) with $Q(\xi) = 0$ when $\lambda^{(0)} = -(N+1)\left[\tau' + \frac{1}{2}N\sigma''\right]$ for a prescribed approximation order N.

4. Roots of the classical orthogonal polynomials

The classical orthogonal polynomials are characterized by the celebrated Rodrigues formula

$$p_n(\xi) = \frac{K_n}{\rho(\xi)}\frac{\mathrm{d}^n}{\mathrm{d}\xi^n}\left[\sigma^n(\xi)\rho(\xi)\right] = k_n\xi^n + \cdots \tag{49}$$

for $n = 0, 1, \ldots$, where $\rho(\xi)$ is a weight function satisfying the Pearson equation $[\rho(\xi)\sigma(\xi)]' = \tau(\xi)\rho(\xi)$. Clearly, k_n is the coefficient of the leading order term, and K_n denotes a renormalization constant which depends on the standardization. For instance, the values of K_n for the Hermite, Laguerre and the Jacobi polynomials are taken as $(-1)^n$, $1/n!$ and $(-\frac{1}{2})^n/n!$, respectively, for historical reasons.

Our aim is to find the roots of $p_n(\xi)$ when $n = N+1$. Instead of $p_n(\xi)$, consider the normalized polynomials $\psi_n(\xi) = p_n(\xi)/h_n$ having the same roots, where h_n is the $L^2(a, b)$ norm of the $p_n(\xi)$, i.e., $h_n^2 = \int_a^b p_n^2(\xi)\rho(\xi)\mathrm{d}\xi$. In [33], Taşeli has expressed the usual three-term recursion for $\psi_n(\xi)$ in the form

$$A_n\psi_{n+1}(\xi) + (B_n - \xi)\psi_n(\xi) + A_{n-1}\psi_{n-1}(\xi) = 0, \quad n = 0, 1, \ldots \tag{50}$$

with the coefficients

$$A_n = \frac{k_n}{k_{n+1}}\frac{h_{n+1}}{h_n} \quad \text{and} \quad B_n = \eta_{n-1} - \eta_n \tag{51}$$

where $A_{-1} \equiv 0$. These coefficients can be identified completely by means of the coefficients in the EHT. Indeed, the ratios k_{n+1}/k_n and h_{n+1}/h_n are expressible as

$$\frac{k_{n+1}}{k_n} = -\frac{K_{n+1}}{K_n}\frac{\lambda^{(0)}_{2n}\lambda^{(0)}_{2n+1}}{2(2n+1)\lambda^{(0)}_n}, \qquad k_0 = K_0 \tag{52}$$

Table 1
The first few eigenvalues of ADWP for $a_1 = 100$, as a function of a_2. The last two columns include the results from MATSLISE and SLEIGN2, respectively, for comparison.

a_2	c_{opt}	N	n	E_n: Present work	E_n: MATSLISE [4]	E_n: SLEIGN2 [2]
0.25	4.4	69	0	−4.277 344 849 182 474 166 847 348 848 02	−4.277 344 849 182 477	−4.277 344 849 171
		69	1	7.080 517 391 364 158 656 090 710 350 21	7.080 517 391 364 156	7.080 517 391 364
		72	2	19.817 761 502 618 821 399 175 325 525 2	19.817 761 502 618 819	19.817 761 502 6
		73	3	36.209 337 296 287 706 584 558 242 608 6	36.209 337 296 287 693	36.209 337 296 497
0.50	4.4	58	0	−6.816 052 047 536 736 982 561 430 365 98	−6.816 052 047 536 741	−6.816 052 047 576
		58	1	4.675 693 930 558 290 057 997 135 848 24	4.675 693 930 558 290	4.675 693 930 56
		59	2	15.973 204 136 317 836 561 600 922 534 7	15.973 204 136 317 833	15.973 204 136 345
		62	3	31.505 546 630 519 551 260 800 075 872 1	31.505 546 630 519 540	31.505 546 630 52
0.75	4.4	57	0	−9.459 479 212 224 512 858 546 562 584 43	−9.459 479 212 224 517	−9.459 479 212 179
		57	1	0.010 560 072 717 619 621 379 801 416 92	0.010 560 072 717 621	0.010 560 072 9
		59	2	10.866 977 233 476 768 562 653 506 503 7	10.866 977 233 476 764	10.866 977 233
		61	3	24.888 991 175 519 381 797 134 001 071 9	24.888 991 175 519 376	24.888 991 176

and

$$\left(\frac{h_{n+1}}{h_n}\right)^2 = 4\left(\frac{k_{n+1}}{k_n}\right)^2 \frac{\lambda_n^{(0)}}{\lambda_{2n+2}^{(0)}\lambda_{2n}^{(0)}}\left[(n+1)^2\sigma(0) - (n+1)\eta_n\sigma'(0) + \frac{1}{2}\eta_n^2\sigma''\right] \tag{53}$$

where the parameter η_n, that also appears in B_n, is given by

$$\eta_{n-1} = n\left[\frac{\tau(0) + (n-1)\sigma'(0)}{\tau' + (n-1)\sigma''}\right] \tag{54}$$

whose proofs can be found in [33].

Running recursion (50) over the range $n = 0, 1, \ldots, N$ we obtain an inhomogeneous linear algebraic system $(\boldsymbol{R} - \xi \boldsymbol{I})\boldsymbol{x} = \boldsymbol{b}$, where

$$\boldsymbol{R} = \begin{bmatrix} B_0 & A_0 & & & 0 \\ A_0 & B_1 & A_1 & & \\ & A_1 & B_2 & \ddots & \\ & & \ddots & \ddots & A_{N-1} \\ 0 & & & A_{N-1} & B_N \end{bmatrix} \tag{55}$$

is a tridiagonal symmetric square matrix of size $N+1$. Notice here that $\boldsymbol{b} = [0, 0, \ldots, 0, A_N\psi_{N+1}(\xi)]^{\mathrm{T}}$ is an $N+1$ vector with only one nonzero component. Therefore, if we set $\psi_{N+1}(\xi) = 0$ or, equivalently, $p_{N+1}(\xi) = 0$ then the system reduces to a standard eigenvalue problem $\boldsymbol{Rx} = \xi\boldsymbol{x}$ with the eigenvalue parameter ξ, which provides us with the roots of $p_{N+1}(\xi)$ as required. Consequently, the nodal points ξ_n in the pseudospectral scheme of Section 3 turn out to be the eigenvalues of the symmetric tridiagonal matrix $\boldsymbol{R}$ defined by (55).

5. Numerical applications and discussion

The pseudospectral algorithm suggested in this article is applied to a set of problems handled in Sections 1 and 2 for various potential functions $V(\xi)$. Recall that EHTP (8) characterizes basically three kinds of problems depending on the degree of the coefficient $\sigma(\xi)$; the cases $\sigma(\xi) = 1, \xi$ and $1-\xi^2$ which have been referred to as the EHTP of the first, second and the third kind, respectively. A few examples falling into the three categories are treated for illustration.

First we consider the EHTP of the first kind in (3) with the asymmetrical double-well potential (ADWP)

$$V(x) = a_1x^2(x+a_2)(x-1), \qquad a_1 > 0,\ 0 < a_2 < 1,\ x \in (-\infty, \infty) \tag{56}$$

which has two minima located asymmetrically about the origin [34]. It is clear that the left hand limiting value of a_2, $a_2 = 0$, does not represent a double-well oscillator any longer where the potential has an inflection point at $x = 0$ while $a_2 = 1$ corresponds to a symmetrical two-well potential. These potentials are of practical interest for the protonic movement of hydrogen-bonded systems [35,34,14].

Obviously, the Hermite method is suitable for addressing this problem, which leads to the diagonalization of the matrix $\mathcal{B}$ in (48) by taking $\sigma(\xi) = 1$, $\tau(\xi) = -2\xi$ and $Q(\xi) = \xi^2 - c^{-2}[a_1(c^{-1}\xi)^2(c^{-1}\xi + a_2)(c^{-1}\xi - 1)]$. Thus the energy levels $E_n = c^2(1+\lambda_n)$ of Schrödinger equation (2) with an ADWP are listed in Table 1, where the range of a_2 is covered by choosing $a_2 = 0.25$, $a_2 = 0.50$ and $a_2 = 0.75$. In all tables, n stands for the eigenvalue index, N the truncation order for which the desired (machine) accuracy of the corresponding eigenvalue is obtained, and c denotes a scaling or an optimization parameter which may be exploited to accelerate the convergence rate of the method. The effect of c on the accuracy of the

Table 2
The convergence rate of E_0 for ADWP, where $a_1 = 100$ and $a_2 = 0.25$, with respect to optimization parameter c when $N = 69$.

c	E_0
1.1	−4.27
2.2	−4.277 344 849 182
3.3	−4.277 344 849 182 474 166 847 34
4.4	−4.277 344 849 182 474 166 847 348 848 02
5.5	−4.277 344 849 182 474 166 847 3
6.6	−4.277 344 84
7.7	−4.277

Table 3
The first few nearly degenerate eigenvalues of SDWP with $N = 60$, $c = 2.05$. The last two columns include the results from MATSLISE and SLEIGN2, respectively, for comparison.

n	E_n: Present work	E_n: MATSLISE [4]	E_n: SLEIGN2 [2]
0	−149.219 456 142 190 888 029 163 966 538	−149.219 456 142 190 8	−149.219 456 142 345
1	−149.219 456 142 190 888 029 163 958 974	−149.219 456 142 190 8	−149.219 456 142 114
2	−135.324 512 011 840 858 579 892 393 334	−135.324 512 011 840 9	−135.324 512 011 826
3	−135.324 512 011 840 858 579 887 397 260	−135.324 512 011 840 9	−135.324 511 213
4	−121.688 950 604 621 648 258 910 138 759	−121.688 950 604 621 6	−121.688 950 608
5	−121.688 950 604 621 648 257 347 725 677	−121.688 950 604 621 6	−121.688 982

Table 4
The convergence rate of E_{100} of the SDWP, where $c = 2.6$.

N	E_{100}
90	625.512 519 838 7
95	625.512 519 838 760 54
100	625.512 519 838 760 543 998
105	625.512 519 838 760 543 998 347 7
110	625.512 519 838 760 543 998 347 757 56
115	625.512 519 838 760 543 998 347 757 560 1
116	625.512 519 838 760 543 998 347 757 560 1

ground state eigenvalue E_0 of an ADWP is displayed in Table 2. Note that we used quadruple-precision arithmetic on a main frame computer with machine accuracy of about 32 digits, by truncating the results to 29–31 significant figures. For comparison, Table 1 also contains eigenvalues calculated by the two algorithms MATSLISE and SLEIGN2, requesting their maximum achievable accuracy. The routines are executed with a double-precision arithmetic (16 digits), and the results are in good agreement with those of the present work to the accuracy quoted. To be specific, MATSLISE gives about 15 correct digits while SLEIGN2 seems to provide only 9-11 figures for the problem being considered.

Next, we discuss the same system (2) with the symmetric double-well potential (SDWP)

$$V(x) = x^4 - 25x^2, \quad x \in (-\infty, \infty) \tag{57}$$

having two minima located symmetrically about the origin. The interesting property of its energy spectrum is that the lower eigenvalues are very closely bunched in pairs if the wells are sufficiently separated. To determine the gap between nearly degenerate eigenvalues of SDWPs, several methods have been proposed such as WKB and JWKB approximations [18–20], finite difference calculation [7], the path-integral approach [22], the recursive series method [21] and the Rayleigh–Ritz variational method [8].

Since the SWDP (57) is even, the EHTP corresponding to this example is (4) having $\sigma(\xi) = \xi$, $\tau(\xi) = \gamma + 1 - \xi$ and $Q(\xi) = \frac{1}{4}\left[\xi - c^{-6}\xi^2 - 25c^{-4}\xi\right]$, for which the Laguerre pseudospectral method becomes appropriate with $\gamma = -\frac{1}{2}$ and $\gamma = \frac{1}{2}$ for the even and odd states, respectively. Therefore, the energy eigenvalues $E_{2n} = c^2(1 + 4\lambda_n)$ and $E_{2n+1} = c^2(3 + 4\lambda_n)$ of the SDWP calculated by this algorithm and those of MATSLISE and SLEIGN2 are listed in Table 3.

From Table 3 it is shown that the matrix size $N = 60$ is sufficient to calculate the first six eigenvalues to the machine accuracy, where the optimization parameter is $c_{\text{opt}} = 2.05$. It is clear that the determination of the gaps requires a high precision algorithm. Again the present results are in agreement with those of MATSLISE and SLEIGN2; however, the gaps between the nearly degenerate states are unclear, especially in SLEIGN2.

In addition, our method gives not only satisfactory results for lower eigenvalues but also for higher states. For instance, in Table 4 we illustrate the convergence rate of E_{100} as a function of the truncation size N. Observe that eigenvalue E_{100} stabilizes when $N = 115$ and $N = 116$. In general, the accuracy of the results in all tables reported here has been checked similarly by inspecting the number of stable digits between two consecutive truncation orders. On the other hand, MATSLISE and SLEIGN2 give the results 625.512 519 838 762 and 625.512 519 835 819 for this eigenvalue, respectively, which are accurate only to 14 and 11 digits.

Table 5
The convergence rate of $E_{0,0}(3)$ for the Gaussian potential as a function of δ. The last column includes some results from the literature for comparison.

δ	c_{opt}	N	$E_{0,0}(3)$										$E_{0,0}(3)$ calculated by other algorithms							
0.001	0.15	10	−0.907	019	292	592														
		15	−0.907	019	292	592	812	08					SLEIGN2 [2]	−0.907	019	290				
		20	−0.907	019	292	592	812	082	715				MATSLISE [4]	−0.907	019	292	592	810		
		27	−0.907	019	292	592	812	082	715	416	167	1	Reference [36]	−0.907	019	292	592	812	082	715	5/0
0.01	0.30	15	−0.719	168	933	445	0													
		25	−0.719	168	933	445	090	397					SLEIGN2 [2]	−0.719	168	936				
		35	−0.719	168	933	445	090	397	309	290			MATSLISE [4]	−0.719	168	933	445	089		
		45	−0.719	168	933	445	090	397	309	290	824	9	Reference [36]	−0.719	168	933	445	090	397	5/0
0.1	0.33	60	−0.254	340	163	216	611	8												
		80	−0.254	340	163	216	611	811	747				SLEIGN2 [2]	−0.254	340	161				
		100	−0.254	340	163	216	611	811	747	716			MATSLISE [4]	Failed.						
		122	−0.254	340	163	216	611	811	747	716	919	8	Reference [36]	Not reported.						

Thirdly, we take into account the radial Schrödinger equation (10) defined over the half-line with the nonpolynomial Gaussian potential

$$V(r) = -\mathrm{e}^{-\delta r^2}, \quad \delta > 0 \tag{58}$$

having a finite number of discrete eigenvalues located on the negative real axis together with a continuous spectrum over the entire positive real axis for small values of the parameter δ. There exist a threshold value δ_{thr}, of the parameter δ, for which the discrete negative spectral points can no longer survive and melt fully into the continuous spectrum. Zafer and Taşeli [36] calculated lower and upper bounds for the discrete states by truncating the usual unbounded domain of the system to a finite interval.

The Laguerre method suggested by EHTP (15) associated with (58) is performed for $\gamma = \frac{1}{2}M + \ell - 1$. Then the energies, denoted by $E_{n,\ell}(M)$, of (10) are given by the simple formula $E_{n,\ell}(M) = c^2(M + 2\ell - 4\lambda_n)$ in terms of the eigenvalues λ of matrix $\boldsymbol{\mathcal{B}}$. In Table 5, we present the convergence rate of the ground state energy $E_{0,0}(3)$ of the vibrational levels $\ell = 0$ of the Gaussian potential in three dimensions $M = 3$ as δ varies. Table 5 exhibits the fact that, as in the other methods [2,4,36], a noticeable slowing down of convergence is encountered for the discrete states just below zero, as δ approaches its threshold value.

We now consider the angular spheroidal wave equation

$$\left\{-\frac{\mathrm{d}}{\mathrm{d}t}\left[(1-t^2)\frac{\mathrm{d}}{\mathrm{d}t}\right] + C^2t^2 + \frac{m^2}{1-t^2}\right\} u(t) = Eu(t), \quad u(t) \in L^2(-1, 1) \tag{59}$$

where the angular momentum m is an integer and the oblateness parameter C real, which results from the Helmholtz equation by separation of variables in the prolate spheroidal coordinates. It arises in different areas of physics such as atomic and molecular physics, light scattering in optics and the nuclear shell model [37]. The asymptotic iteration method is applied to calculate the angular spheroidal eigenvalues $E_n(m, C^2)$ by Barakat et al. [37]. Miyazaki et al. [38] and Volkmer [39] proposed a matrix method and a Rayleigh–Ritz approximation, respectively, for computing the eigenvalues which obtained precise and explicit error estimates for the approximated eigenvalues as well.

Actually, the spheroidal wave equation is no more than system (17) with $V(\sin\theta) = C^2\sin^2\theta$, whenever the inverse substitution

$$\theta = \arcsin t, \quad \theta \in \left(-\frac{1}{2}\pi, \frac{1}{2}\pi\right) \tag{60}$$

is applied to the spheroidal wave equation in (59). Therefore, the EHTPs corresponding to the even and odd states of (59) are (23) and (26) with $V(\sqrt{(1-\xi)/2}) = C^2(1-\xi)/2$, respectively, which suggest the use of the Jacobi pseudospectral methods having the parameter sets $\{\alpha, \beta\} = \{-\frac{1}{2}, m\}$ and $\{\frac{1}{2}, m\}$. Thus the eigenvalues of the spheroidal wave equation, $E_{2n}(m, C^2) = m(m+1)+4\lambda_n$ and $E_{2n+1}(m, C^2) = (m+1)(m+2)+4\lambda_n$ are given in Table 6. It demonstrates the convergence rates of several states with $m = 0$ and $C^2 = 10$. The extremely fast convergence rate of the method for an arbitrary state number n is quite impressive. Moreover, in Table 7, we compare the truncation sizes necessary to obtain the ground state energy with the prescribed accuracy as m and C^2 vary. It is observed that the increase in the angular quantum number m causes the decrease in the matrix size N whereas the increase in the oblateness parameter C^2 implies an increment in N.

The last example is the Schrödinger equation with a periodic potential

$$\left[-\frac{\mathrm{d}^2}{\mathrm{d}\zeta^2} + V(\cos 2\zeta)\right]\Theta(\zeta) = E\Theta(\zeta), \quad \zeta \in \left(-\frac{1}{2}\pi, \frac{1}{2}\pi\right) \tag{61}$$

subject to the conditions $\Theta\left(\pm\frac{\pi}{2}\right) = 0$. Rescaling the independent variable by putting $\theta = 2\zeta$, we obtain an equivalent equation

Table 6
The convergence rate of eigenvalues $E_n(0, 10)$ of the spheroidal wave equation as n varies.

N	$E_0(0, 10)$	N	$E_{100}(0, 10)$
5	2.305 040 10	51	10105.0
6	2.305 040 107 940	52	10105.000 433
7	2.305 040 107 940 431 6	53	10105.000 433 246 48
8	2.305 040 107 940 431 635 6	54	10105.000 433 246 482 907 99
9	2.305 040 107 940 431 635 679 732	55	10105.000 433 246 482 907 993 562 45
10	2.305 040 107 940 431 635 679 732 102 9	56	10105.000 433 246 482 907 993 562 450 0
11	2.305 040 107 940 431 635 679 732 102 9	57	10105.000 433 246 482 907 993 562 450 0
N	$E_{200}(0, 10)$	N	$E_{400}(0, 10)$
101	40205.00	201	160405.00
102	40205.000 108 8	202	160405.000 027 2
103	40205.000 108 835 777	203	160405.000 027 275 870 8
104	40205.000 108 835 777 578 646 2	204	160405.000 027 275 870 838 131 19
105	40205.000 108 835 777 578 646 209 290	205	160405.000 027 275 870 838 131 198 65
106	40205.000 108 835 777 578 646 209 290	206	160405.000 027 275 870 838 131 198 65

Table 7
Truncation sizes for calculating $E_0(m, C^2)$ to the machine accuracy as functions of m and C^2.

C^2	N for $m = 0$	N for $m = 10$	m	N for $C^2 = 10$	N for $C^2 = 100$
1	7	5	1	9	15
10	10	7	10	7	11
100	15	11	100	4	6
1000	25	20	1000	3	6
10000	42	38	10000	2	5

$$\left[-\frac{\mathrm{d}^2}{\mathrm{d}\theta^2}+\frac{1}{4}V(\cos\theta)\right]\Theta(\theta)=\frac{1}{4}E\Theta(\theta),\quad \Theta(\pm\pi)=0 \tag{62}$$

which is the limiting case of (27) when $\mu \to 0^+$ with $V(\cos\theta)$ and E scaled by $\frac{1}{4}$. Therefore, the EHTPs of the third kind corresponding to even and odd states are written from (28) and (29),

$$(1-\xi^2)y''+(1-2\xi)y'-\frac{1}{4}V(\xi)y=-\lambda y,\qquad E_{2n}=1+4\lambda_n \tag{63}$$

and

$$(1-\xi^2)y''-3\xi y'-\frac{1}{4}V(\xi)y=-\lambda y,\qquad E_{2n+1}=4(1+\lambda_n) \tag{64}$$

respectively, where $\{\alpha, \beta\} = \{-\frac{1}{2}, \frac{1}{2}\}$ and $\{\frac{1}{2}, \frac{1}{2}\}$.

Well-known particular cases of (61) are the Mathieu and Coffey–Evans equations, if $V(\cos 2\zeta) = 2q\cos 2\zeta$ and $V(\cos 2\zeta) = \nu^2 \sin^2 2\zeta - 2\nu\cos 2\zeta$, respectively, where q and ν denote real parameters. The parameter ν in the Coffey–Evans equation controls the depth of the well potential under consideration. As ν increases, nearly degenerate triple states may occur. Ledoux et al. [4] prepared the Matlab package MATSLISE for numerical solution of Sturm–Liouville eigenvalue problems including the Mathieu and Coffey–Evans equations by high order piecewise constant perturbation methods. There is other software SLEDGE based on the stabilized shooting method developed in [40].

From (63) and (64), several eigenvalues of the Schrödinger equation in (61) with Mathieu and Coffey–Evans potentials are reported in Tables 8 and 9, respectively, only for the parameter values of $q = 1$ and $\nu = 50$ in order not to overfill the content of the paper with tabular material any further. In fact, the convergence properties of the algorithm in the Mathieu case are typically the same for all q although a slight slowing down of convergence is observed as q increases. A truncation order of $N = 72$ suffices to get the reported accuracy in Table 9 for the low lying states of the Coffey–Evans equation. It is shown that, as for the symmetric double-well oscillator over the real line, the method is capable of determining the gaps between the nearly degenerate triple states of the Coffey–Evans equation successfully. Clustering of the eigenvalues does not seem to cause any difficulties in computations which is a serious trouble for many other methods [41]. Moreover, when high accuracy is required, the above codes [4,40] have to work hard on some of the triplets to produce reasonable results.

We report also in Table 8 eigenvalues of the Mathieu equation calculated by MATSLISE and SLEIGN2 for comparison. It is shown that our results are in excellent agreement with those of MATSLISE. SLEIGN2 is, on the other hand, accurate to 9–11 digits and fails to compute the eigenvalues E_n with a high quantum number n, typically when $n > 310$. To sum up, we observe that MATSLISE yields in general 15–16 correct digits, which is the machine accuracy of the algorithm that uses double-precision arithmetic. Then, one can argue that it could reach the precision of the present method if it were executed in the quadruple-precision arithmetic. On the other hand, this is probably not the case for SLEIGN2. Clearly, SLEIGN2 cannot

Table 8
Several eigenvalues of Mathieu differential equation with $q = 1$. The last two columns include the results from MATSLISE and SLEIGN2, respectively, for comparison.

n	N	E_n: Present work	E_n: MATSLISE [4]	E_n: SLEIGN2 [2]
0	9	−0.110 248 816 992 095 169 906 547 85	−0.110 248 816 992 095	−0.110 248 816 990 864
100	55	10201.000 049 019 607 990 453 093 342 0	10201.000 049 019 61	10201.000 048 997 7
200	105	40401.000 012 376 237 626 132 297 845 2	40401.000 012 376 22	40401.000 012 279 6
300	154	90601.000 005 518 763 797 119 609 337	90601.000 005 518 73	90601.000 004 267 9
400	204	160801.000 003 109 452 736 355 989 67	160801.000 003 109	Failed
500	254	251001.000 001 992 031 872 519 841 33	251001.000 001 992	Failed
1000	504	1002001.000 000 499 001 996 008 139 4	1002001.000 000 499	Failed

Table 9
Triple eigenvalues of the Coffey–Evans equation with $\nu = 50$, $N = 72$.

n	E_n	n	E_n
0	0.000 000 000 000 000 000 000 000 0	9	947.047 491 585 860 179 592 142 658 2
1	197.968 726 516 507 291 450 189 104 5	10	1122.762 920 067 901 205 616 045 550 3
2	391.808 191 489 053 841 050 234 434 6	11	1122.762 920 071 056 526 891 891 942 2
3	391.808 191 489 053 841 832 241 249 9	12	1122.762 920 074 211 848 168 115 209 4
4	391.808 191 489 053 842 614 248 065 8	13	1293.423 567 331 707 081 413 958 872 2
5	581.377 109 231 579 654 864 715 898 8	14	1458.746 557 025 357 659 317 371 063 0
6	766.516 827 285 532 616 579 817 794 1	15	1458.746 558 472 128 708 810 534 887 1
7	766.516 827 285 535 505 431 430 237 3	16	1458.746 559 918 899 832 786 248 167 6
8	766.516 827 285 538 394 283 042 681 3	17	1618.391 008 042 643 345 932 885 816 0

Table 10
Comparison with the standard Chebyshev Pseudospectral Method (CPM) for the first eigenvalue of the Mathieu equation with $q = 1$.

N_{CPM}	E_0	N	E_0
7	−0.10	2	−0.10
14	−0.110 248 4	3	−0.110 248 4
20	−0.110 248 817 3	4	−0.110 248 816 9
27	−0.110 248 816 991 9	5	−0.110 248 816 992 08

reach the 16-digit machine accuracy, giving only 9-11 significant figures. So increasing the precision of computer arithmetic does not seem to improve the results considerably, at least for the problems being considered here.

In this paper, we present a unified pseudospectral framework based on the classical orthogonal polynomials for computing the eigenvalues of a wide class of physical problems, which can be transformed into an EHTP. A symmetric matrix representation of the differential eigenvalue problem is formulated, where the matrix elements are determined using simple and elegant analytical expressions. In this setting the collocation points are also computed numerically to an arbitrary precision as the eigenvalues of a tridiagonal symmetric matrix.

One of the most commonly used methods in the literature is the Chebyshev pseudospectral method, which has two main practical advantages. First the zeros of the Chebyshev polynomials are expressible in closed form, and the second kth differentiation matrix $\boldsymbol{D}^{(k)}$ can be obtained from $\boldsymbol{D}^{(1)}$ by taking its kth power. Nevertheless, our approach enables us to work automatically with the best appropriate classical orthogonal polynomial in the construction of the Lagrange interpolation, depending on the specific structure of the problem in question. For example, our algorithm suggests the use of the Jacobi polynomial $P_{N+1}^{(-\frac{1}{2},\frac{1}{2})}(\xi)$ for the even states of the Mathieu equation. If the standard Chebyshev method is used directly, then the loss of accuracy is as illustrated in Table 10. To be specific, to compute the ground state of the Mathieu equation accurate approximately to 10 digits the standard Chebyshev method requires the diagonalization of a matrix of order $N_{CPM} = 27$ whereas the same accuracy is reached at $N = 5$ in our algorithm. Actually, this is typical for all problems considered in this study.

We have taken advantage of the Hermite, Laguerre and the Jacobi pseudospectral methods for the problems over the real line, half-line and finite intervals, respectively. Numerical results verify the exponential rate of convergence, as expected theoretically for spectral methods [42]. Recall also that the separation of even and odd states of reflection symmetric systems, such as (28) and (29) of (27) provides an additional numerical advantage of dealing with two matrices of order N rather than a matrix of order $2N$.

Finally, the convergence of the Hermite and Laguerre pseudospectral methods may be accelerated by a scaling transformation. There exists an optimum value of the scale factor c in (3) for which the desired accuracy is achieved at the smallest possible matrix size N. From Table 2 we notice that at a fixed truncation size of $N = 69$, E_0 converges to 30 digits when $c = 4.4$ whereas at the same truncation size we get merely three or four correct digits when $c = 1.1$ and $c = 7.7$, respectively. The optimum value of c can be estimated by inspecting the actual solution or, at least, its asymptotic behavior if it is known in advance [43]. Otherwise it can be determined roughly by numerical experiments, i.e. by the trial and error technique. In this process, if a user takes a "bad" value for c then either the algorithm diverges or the convergence is

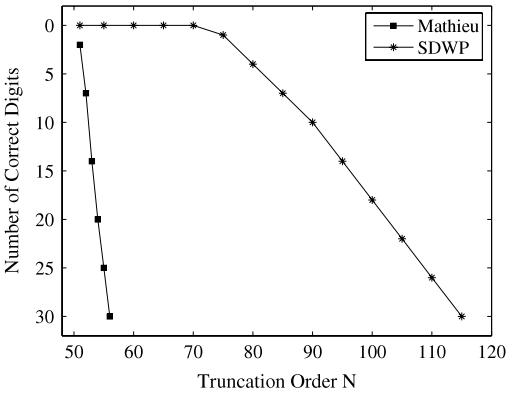

Fig. 1. Number of correct digits versus matrix size N for E_{100} of Mathieu equation with $q = 1$, and SDWP in (57).

reached at the cost of employing very high truncation orders N. In fact, a scaling transformation maps unbounded intervals onto themselves by solely rescaling the location of the points in the interval, whereas it is useless for the finite interval problems since it just shrinks or stretches the whole picture. In spite of the existence of such an optimization parameter in the Hermite and Laguerre methods the convergence is still slower when compared to the Jacobi pseudospectral methods. In Fig. 1, we demonstrate how quickly the accuracy is improved as N increases in a typical Jacobi and a Laguerre method.

Acknowledgement

This research was supported by a grant from TÜBİTAK, the Scientific and Technological Research Council of Turkey.

References

[1] J. Killingbeck, Shooting methods for the Schrödinger equation, J. Phys. A: Math. Gen. 20 (1987) 1411–1417.
[2] P.B. Bailey, W.N. Everitt, A. Zettl, Algorithm 810: The SLEIGN2 Strum–Liouville code, ACM Trans. Math. Softw. 27 (2001) 143–192.
[3] P.B. Bailey, B.S. Garbow, H.G. Kaper, A. Zettl, Eigenvalue and eigenfunction computations for Strum–Liouville problems, ACM Trans. Math. Softw. 17 (1991) 491–499.
[4] V. Ledoux, M. Van Daele, G. Vanden Berghe, MATSLISE: A MATLAB package for the numerical solution of Strum–Liouville and Schrödinger equation, ACM Trans. Math. Softw. 31 (2005) 532–554.
[5] V. Ledoux, M. Van Daele, G. Vanden Berghe, CP methods of higher order for Sturm–Liouville and Schrödinger equations, Comput. Phys. Comm. 162 (2004) 151–165.
[6] V. Fack, G. Vanden Berghe, A Finite difference approach for the calculation of perturbed oscillator energies, J. Phys. A: Math. Gen. 18 (1985) 3355–3363.
[7] M.R.M. Witwit, Finite difference calculations of eigenvalues of various potentials, J. Phys. A: Math. Gen. 25 (1992) 503–512.
[8] H. Taşeli, M.B. Erseçen, The scaled Hermite–Weber basis still highly competitive, J. Math. Chem. 34 (2003) 177–188.
[9] H. Taşeli, Modified Laguerre basis for hydrogen-like systems, Int. J. Quantum Chem. 63 (1997) 949–959.
[10] H. Taşeli, A. Zafer, A Fourier–Bessel expansion for solving radial Schrodinger equation in two dimensions, Int. J. Quantum Chem. 61 (1997) 759–768.
[11] H. Taşeli, M. Demiralp, Studies on algebraic methods to solve linear eigenvalue problems: Generalized anharmonic oscillators, J. Phys. A: Math. Gen. 21 (1988) 3903–3919.
[12] A.N. Drozdov, On the improvement of convergence of Hill determinants, J. Phys. A: Math. Gen. 28 (1995) 445–457.
[13] M.R.M. Witwit, J.P. Killingbeck, A Hill-determinant approach to symmetric double-well potentials in two dimensions, Can. J. Phys. 73 (1995) 632–637.
[14] M. Znojil, Asymmetric anharmonic oscillators in the Hill determinant picture, J. Math. Phys. 33 (1992) 213–221.
[15] K. Banerjee, General anharmonic oscillators, Proc. R. Soc. Lond. A 364 (1978) 265–275.
[16] R.N. Keserwani, Y.P. Varshni, Eigenvalues of an anharmonic oscillator, J. Math. Phys. 22 (1981) 1983–1989.
[17] J. Killingbeck, A hypervirial JWKB calculation, J. Phys. A: Math. Gen. 20 (1987) 601–606.
[18] R.F. Dashen, B. Hasslacher, A. Neveu, Nonperturbative methods and extended-hadron models in field theory. I. semiclassical functional methods, Phys. Rev. D 10 (1974) 4114–4129.
[19] C.S. Hsue, J.L. Chern, Two step approach to one-dimensional anharmonic oscillators, Phys. Rev. D 29 (1984) 643–647.
[20] A.M. Sanches, J.D. Bejarano, Quantum anharmonic symmetrical oscillators using elliptic functions, J. Phys. A: Math. Gen. 19 (1986) 887–902.
[21] K. Banerjee, S.P. Bhatnagar, Two well oscillators, Phys. Rev. D 18 (1978) 4767–4769.
[22] E. Gildener, A. Patrascioui, Pseudo particle contributions to the energy spectrum of a one dimensional system, Phys. Rev. D 16 (1977) 423–430.
[23] H. Chen, B.D. Shizgal, The Quadrature Discretization Method (QDM) in the solution of the Schrodinger equation, J. Math. Chem. 24 (1998) 321–343.
[24] J. Lo, B.D. Shizgal, Spectral convergence of the quadrature discretization method in the solution of the Schrödinger and Fokker–Planck equations: Comparison with sinc methods, J. Chem. Phys. 125 (2006) 194108.1–194108.17.
[25] H. Taşeli, H. Alıcı, The scaled Hermite–Weber basis in the spectral and pseudospectral pictures, J. Math. Chem. 38 (2005) 367–378.
[26] H. Taşeli, H. Alıcı, The Laguerre pseudospectral method for the reflection symmetric Hamiltonians on the real line, J. Math. Chem. 41 (2007) 407–416.
[27] J.A.C. Weideman, Spectral differentiation matrices for the numerical solution of Schrödinger's equation, J. Phys. A: Math. Gen. 39 (2006) 10229–10237.
[28] A.F. Nikiforov, V.B. Uvarov, Special Functions of Mathematical Physics, Birkhäuser, Basel, 1988.
[29] G. Michael, On a singular Sturm–Liouville problem in the theory of molecular vibrations, J. Math. Chem. 39 (2006) 523–539.
[30] M.G. Marmorino, Exactly soluble Hamiltonian with a squared cotangent potential, J. Math. Chem. 32 (2002) 303–308.
[31] H. Taşeli, Exact analytical solutions of the Hamiltonian with a squared tangent potential, J. Math. Chem. 34 (2003) 243–251.
[32] D. Funaro, Polynomial Approximations of Differential Equations, Springer-Verlag, Berlin, 1992.
[33] H. Taşeli, A unification of recursions for functions of the hypergeometric type (submitted for publication).
[34] H. Taşeli, Accurate lower and upper bounds of the energy spectrum for the asymmetrical two-well potentials, Int. J. Quantum Chem. 60 (1996) 641–648.
[35] R.L. Somorjai, D.F. Hornig, Double-minimum potentials in hydrogen-bonded solids, J. Chem. Phys. 36 (1962) 1980–1987.

[36] A. Zafer, H. Taşeli, Two-sided eigenvalue bounds for the spherically symmetric states of the Schrödinger equation, J. Comput. Appl. Math. 95 (1998) 83–100.
[37] T. Barakat, K. Abodayeh, A. Mukheimer, The asymptotic iteration method for the angular spheroidal eigenvalues, J. Phys. A: Math. Gen. 38 (2005) 1299–1304.
[38] Y. Miyazaki, N. Asai, D. Cai, Y. Ikebe, Numerical computation of the eigenvalues for the spheroidal wave equation with accurate error estimation by matrix method, ETNA 23 (2006) 329–338.
[39] H. Volkmer, Error estimates for Rayleigh Ritz approximations of eigenvalues and eigenfunctions of the Mathieu and spheroidal wave equation, Constr. Approx. 20 (2004) 39–54.
[40] S. Pruess, C.T. Fulton, Mathematical software for Sturm–Liouville problems, ACM Trans. Math. Softw. 19 (1993) 360–376.
[41] J.D. Pryce, Numerical Solution of Sturm–Liouville Problems, Oxford University Press, 1993.
[42] C. Canuto, M.Y. Hussaini, A. Quarteroni, T.A. Zang, Spectral Methods Fundamentals in Single Domains, Springer-Verlag, Berlin, Heidelberg, 2006.
[43] T. Tang, The Hermite spectral method for Gaussian-type functions, SIAM J. Sci. Comput. 14 (1993) 594–606.